Cellular Signalling 26 (2014) 1226–1234

Contents lists available at ScienceDirect

Cellular Signalling

journal homepage: www.elsevier.com/locate/cellsig

The eIF2B-interacting domain of RGS2 protects against GPCR agonist-induced hypertrophy in neonatal rat cardiomyocytes

Peter Chidiac [a], Alina J. Sobiesiak [a], Katherine N. Lee [a], Robert Gros [a], Chau H. Nguyen [a,b,*]

[a] Department of Physiology and Pharmacology, Schulich School of Medicine and Dentistry, University of Western Ontario, London, ON N6A 5C1, Canada
[b] School of Pharmacy, D'Youville College, Buffalo, NY 14201, USA

ARTICLE INFO

Article history:
Received 27 August 2013
Received in revised form 5 February 2014
Accepted 11 February 2014
Available online 24 February 2014

Keywords:
RGS protein
Cardiac hypertrophy
G protein
GPCR
Protein synthesis

ABSTRACT

The protective effect of Regulator of G protein Signaling 2 (RGS2) in cardiac hypertrophy is thought to occur through its ability to inhibit the chronic GPCR signaling that promotes pathogenic growth both *in vivo* and in cultured cardiomyocytes. However, RGS2 is known to have additional functions beyond its activity as a GTPase accelerating protein, such as the ability to bind to eukaryotic initiation factor, eIF2B, and inhibit protein synthesis. The RGS2 eIF2B-interacting domain ($RGS2^{eb}$) was examined for its ability to regulate hypertrophy in neonatal ventricular myocytes. Both full-length RGS2 and $RGS2^{eb}$ were able to inhibit agonist-induced cardiomyocyte hypertrophy, but $RGS2^{eb}$ had no effect on receptor-mediated inositol phosphate production, cAMP production, or ERK 1/2 activation. These results suggest that the protective effects of RGS2 in cardiac hypertrophy may derive at least in part from its ability to govern protein synthesis.

1. Introduction

Pathological cardiac hypertrophy is an enlargement of the heart accompanying many forms of heart disease, and is an independent risk factor for cardiovascular morbidity and mortality [1]. In response to a variety of stimuli including chronic hypertension and acute myocardial infarction, the myocardium increases in size in an attempt to normalize wall stress and maintain cardiac function [1,2]. Although initially believed to be a compensatory mechanism, prolonged hypertrophic stimuli can tip the balance from an adaptive towards a maladaptive response, leading to abnormal metabolic, structural, and functional changes that over time can result in cardiac remodeling, increased cardiac fibrosis, dilation and ultimately heart failure [1,2]. As cardiac hypertrophy progresses, cardiomyocytes undergo increased protein synthesis and become larger [3], and also exhibit characteristic genetic changes [4] and signs of ER stress [5].

G-protein coupled receptor (GPCR) signaling regulates essential functions in the cardiovascular system such as heart rate and contractility; however, sustained stimulation of certain G protein-coupled receptors promotes cardiomyocyte hypertrophy and thus plays a pivotal role in the development of human heart failure. These include angiotensin II, endothelin, and α1-adrenergic receptors, which couple primarily to Gq, and also β-adrenergic receptors that primarily activate Gs [6,7]. GPCRs and G proteins are themselves under the control of another family of proteins, the Regulator of G protein Signaling (RGS) proteins [8,9]. RGS proteins are negative modulators of cellular signaling that function by acting as GTPase accelerating proteins (GAP) for members of the Gαi and/or Gαq subfamilies of heterotrimeric G proteins [8–10]. In addition, RGS proteins have also been shown to block signal transduction by interfering with G protein–effector interactions [8–10].

RGS2 is unique among RGS proteins in being Gαq/11-selective [11,12], which results from its low affinity for Gαi [13]. Although it has no observable effect on the GTPase activity of Gαs [11,14], RGS2 is able to inhibit Gαs-stimulated adenylyl cyclase activity [15]. Apart from its effects on G protein-mediated signaling, RGS2 can also regulate tubulin polymerization [16], TRPV6 cation channels [17], and the initiation of mRNA translation [18]. RGS2 inhibits translation *via* its effects on the initiation factor eIF2B, which results in a reduction in global protein synthesis [18]. This function maps to a 37 amino acid residue domain that overlaps extensively with the RGS domain of RGS2 (RGS2 eIF2B-interacting domain), and a corresponding peptide is able to inhibit *in vitro* translation in a dose-dependent manner [18].

RGS2 is upregulated in response to, and can inhibit both Gq- and Gs-mediated signals [15,19–22]. Additionally, RGS2 is upregulated in many cells due to various forms of stress and may contribute to the cellular stress response [23]. RGS2 can impede Gq- and Gs-associated hypertrophic growth in cardiomyocytes, and its loss contributes to the development of hypertrophy [19,20,22,24,25]. Notably, mice lacking RGS2 that undergo transverse aortic constriction exhibit a greater degree of cardiac enlargement and develop heart failure more rapidly than their wild type counterparts [25]. The observed protective effects of RGS2 against hypertrophy are generally assumed to reflect its ability to limit

* Corresponding author at: D'Youville College School of Pharmacy, 320 Porter Avenue, Buffalo, NY 14201, USA. Fax: +1 716 829 8436.
E-mail address: nguyenc@dyc.edu (C.H. Nguyen).

http://dx.doi.org/10.1016/j.cellsig.2014.02.006
0898-6568/

GPCR signaling, however the possible contributions of its other functions have not been explicitly considered. Specifically, the ability of RGS2 to limit global protein synthesis would be expected to limit cellular growth, and in the present study we test the hypothesis that the 37 amino acid eIF2B-interacting domain of RGS2 ($RGS2^{eb}$) might decrease GPCR-induced cardiomyocyte hypertrophy.

The primary factor controlling the physical growth associated with myocardial hypertrophy is regulation of protein synthesis in cardiomyocytes [26], and it has been shown that β-adrenergic receptor-induced hypertrophy is mediated through eIF2Bε [27]. Here we report that both RGS2 and $RGS2^{eb}$ are able to inhibit α- and β-adrenergic receptor-induced hypertrophy in rat neonatal cardiomyocytes. Unlike the full length protein, $RGS2^{eb}$ did not inhibit G protein-mediated effects on second messenger levels or ERK phosphorylation, suggesting that its antihypertrophic effects are due to the direct inhibition of mRNA translation. It follows that the antihypertrophic effect of full length RGS2 may arise at least in part from its ability to curtail protein synthesis.

2. Material and methods

2.1. Recombinant adenoviruses

Replication-defective adenoviruses encoding GFP (Ad-GFP), RGS2 (Ad-RGS2), and the 37 amino acid residue eIF2Bε binding domain of RGS2 (Ad-$RGS2^{eb}$) were generated with the AdMax adenovirus vector creation kit according to the manufacturer's protocol (Microbix Biosystems, Inc., Toronto, Canada). Empty adenovirus (Ad-Ctr) lacking a gene insert was also used as a control. AdEasy Viral Titer kit (Agilent Technologies) was used to determine adenoviral titers following the manufacturer's procedure.

2.2. Isolation and primary cell culture of neonatal rat ventricular myocytes

Neonatal ventricular myocytes were isolated from 1 day-old Sprague–Dawley rats, as adapted from our previous protocol [20,22]. Hearts were removed from neonatal rats and atrial and connective tissue was excised. Hearts were minced into 1 mm pieces and then subjected to 5 rounds of enzymatic digestion for 8–10 min with collagenase II (0.5 mg ml^{-1}; Worthington Biochemical Corporation). Digestion was stopped with an equal volume of Hank's balanced salt solution containing 20% fetal bovine serum (FBS) (Gibco). The cell suspension was centrifuged for 5 min at 2000 ×g and the resulting pellet was resuspended in Dulbecco's Modified Eagle Medium:Nutrient Mixture F12 (DMEM/F12) containing 10% FBS. Cells were preplated in T75 flasks to reduce non-myocyte contamination (Corning) for 90 min. Isolated cardiac myocytes were plated in DMEM/F12 containing 10% FBS, 1× insulin–transferin–selenium Liquid Media Supplement (ITS, Sigma-Aldrich) and penicillin–streptomycin (Invitrogen) at a density of 4×10^5 cells/well of a 6-well dish and maintained at 37 °C and 5% CO_2. Cardiomyocyte cultures were found to be ≥95% pure, as tested by immunofluorescent staining for sarcomeric α-actinin.

2.3. Adenoviral infection of neonatal rat ventricular myocytes

Cardiac myocytes were infected with adenovirus encoding GFP, full-length RGS2, $RGS2^{eb}$, or an empty adenoviral vector (Ad-Ctr) as a control 24 h post-isolation, as adapted from previous studies [20,22]. Adenoviral gene transfer was accomplished by introducing a minimal amount of DMEM/F12 with 2% FBS and penicillin–streptomycin (Invitrogen) (0.5 ml for 6-well plates) containing either increasing concentrations of adenovirus for adenoviral expression experiments (MOI of 1 to 10) or at an MOI of 10 for all other procedures (Fig. 1). After 2 h, the full volume of culture medium containing 10% FBS was added (2 ml per well of 6-well plate) and the myocytes were then incubated for 24 or 48 h at 37 °C and 5% CO_2. Expression of polyhistidine-tagged RGS2 constructs was verified by immunofluorescent staining as well as dot-blot analysis of whole cell lysates (Fig. 1B, C).

2.4. Immunocytochemistry

Cardiomyocytes were seeded on cover slips precoated with 1% collagen solution (Sigma-Aldrich). Following infection and/or treatment, cells were fixed in 4% paraformaldehyde for 15 min, permeabilized with 0.1% Triton X-100 in phosphate-buffered saline (PBS) for 10 min, and blocked with 3% bovine serum albumin (BSA) in PBS for 1 h. They were then incubated overnight at 4 °C in 1% BSA/PBS containing primary antibodies against polyhistidine (His-probe H-15, Santa Cruz Biotechnology Inc., 1:500) or sarcomeric α-actinin (polyclonal anti-α actinin, clone EA-53, Sigma-Aldrich, 1:500), followed by incubation for 1 h with AlexaFluor488 or AlexaFluor594-conjugated secondary antibodies (goat anti-rabbit [Invitrogen, 1:5000] and goat anti-mouse [Invitrogen, 1:500]). Cover slips were visualized using an Olympus ix81 microscope and In Vivo software (Media Cybernetics).

2.5. Drug treatments

To stimulate cardiomyocyte hypertrophy, cells that had been infected with Ad-Ctr, Ad-RGS2 or Ad-$RGS2^{eb}$ were serum-starved overnight and then treated with agonist to activate either α1-adrenergic receptors (phenylephrine (PE) 10 μM, Sigma-Aldrich) or β-adrenergic receptors (Isoproterenol (ISO) 10 μM, Sigma-Aldrich®) for 24 h.

2.6. Measurement of cell surface area

Cellular hypertrophy was assessed by measuring the cellular surface area of sarcomeric α-actinin-stained myocytes, as described above. Cover slips were visualized using an Olympus ix81 microscope using 20× magnification and surface area was quantified using ImagePro Analyzer software (Media Cybernetics) by imaging the boundary of at least 50 randomly-chosen individual cells per condition, averaged, and then normalized to an *n* value of 1. Results are presented as means ± S.E.M. from three independent experiments.

2.7. [^{3}H]-leucine incorporation

De novo protein synthesis in adenovirus-infected cells was assessed by [^{3}H]-leucine incorporation [20,22]. Following serum starvation, cardiomyocytes were treated with the indicated agonists in the presence of [^{3}H]-leucine (37 kBq ml^{-1}, Amersham, GE Healthcare) for 24 h. Cells were then washed 3 times with ice-cold PBS and proteins were precipitated by adding 5% trichloroacetic acid (TCA) and incubating for 1 h on ice. After two additional washes with 5% TCA, cell precipitates were solubilized in 0.2 N NaOH and the radioactivity of [^{3}H]-leucine incorporated into proteins was measured using a liquid scintillation counter (Tri-Carb 2900TR).

2.8. RNA isolation and quantitative RT-PCR

RNA was isolated from neonatal ventricular myocytes using Trizol reagent (Invitrogen) and first strand cDNA synthesis was performed using High Capacity cDNA Reverse Transcription Kit (Applied Biosystems) according to the manufacturer's protocol. Reverse transcribed RNA was subjected to real-time PCR using Taqman Universal PCR master mix; FAM-labeled Taqman expression assay for the genetic markers of hypertrophy: atrial natriuretic peptide, α-skeletal actin, and β-myosin heavy chain; and VIC-labeled Taqman expression assay for GAPDH (Applied Biosystems). Relative cDNA levels were quantified using a standard curve of the respective genes and normalized to GAPDH mRNA measured in parallel.

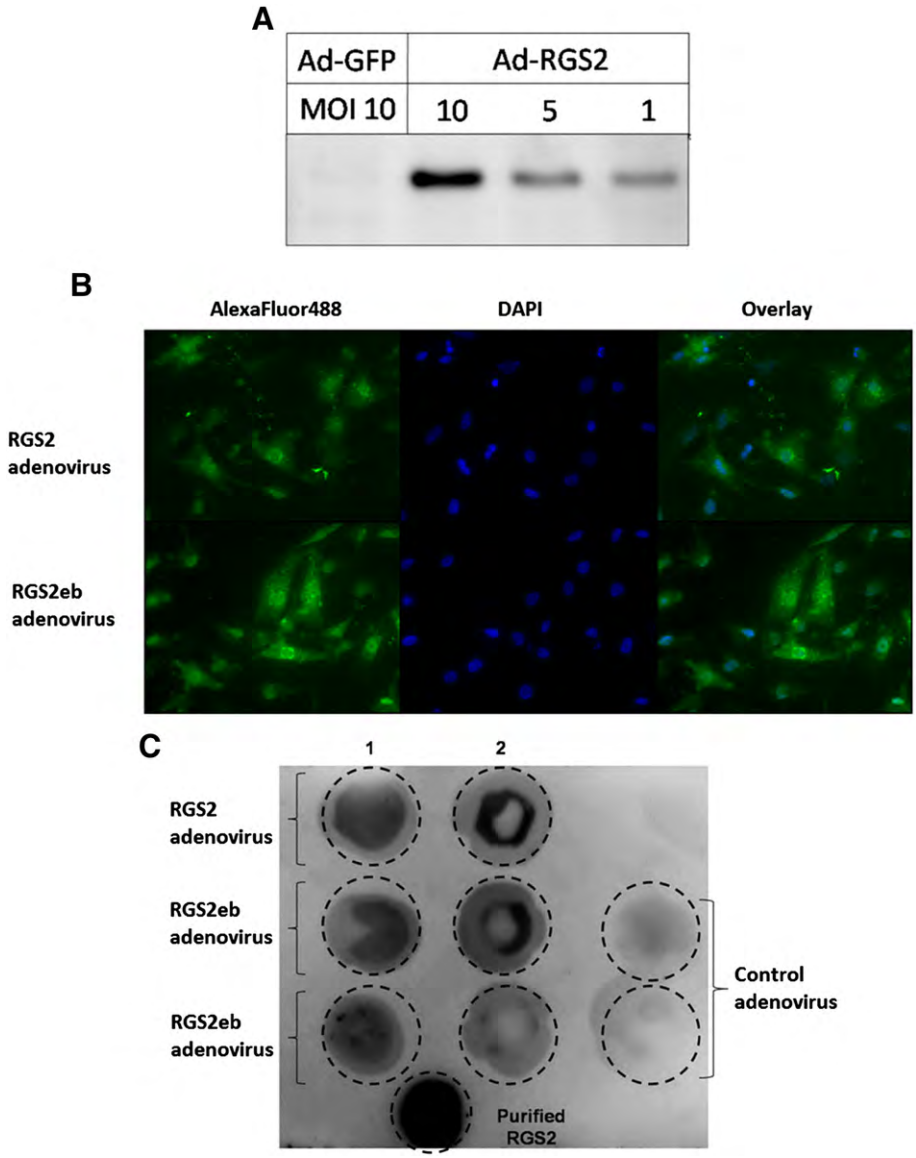

Fig. 1. Expression of adenoviral encoded proteins. (A) Western blot of cell lysates (30 μg/lane) from NVM infected with increasing amounts of Ad-RGS2 for 48 h were probed with anti-His antibody. RGS2 expression increases in a dose-dependent manner with increasing multiplicity of infection (MOI). (B) Adenoviral expression of RGS2 and RGS2^{eb}. NVM were infected with adenovirus at an MOI of 10 for 24 h and immunofluorescently stained with anti-His and AlexaFluor488-conjugated antibodies. DAPI images are shown to indicate efficiency of adenoviral infection (≥95% at an MOI of 10). Shown is a representative of 3 independent experiments. (C) Dot blot of cell lysates from NVM infected with Ad-RGS2, Ad-RGS2^{eb}, or Ad-Ctr for 48 h and probed with anti-His antibody. Purified histidine-tagged RGS2 was spotted on as a positive control.

2.9. Immunoblotting

Rat neonatal ventricular myocytes were infected with adenovirus encoding Ad-Ctr, Ad-RGS2 or Ad-RGS2^{eb} for either 24 or 48 h. For MAPK activation experiments, cardiomyocyte cultures were serum-starved overnight prior to drug treatment. After the indicated treatments, myocytes were rinsed twice with ice-cold PBS and lysed in buffer (20 mM Tris, 150 mM NaCl, 1% Triton X-100, 10% glycerol, 2 mM EDTA, 2 mM EGTA, 50 mM NaF, 200 μM Na_3VO_4, 10 mM $Na_4P_2O_7$, 40 mM β-glycerophosphate, 10 μg ml^{-1} leupeptin, 1 μM pepstatin A, 1 mM PMSF, and 1 μM calyculin A). Cell lysates were held on ice for 30 min and then centrifuged at 10,000 ×g in a microcentrifuge at 4 °C for 15 min. Samples were placed in boiling water for 5 min and equal amounts of protein were subjected to 12% SDS-PAGE. Proteins were then transferred to polyvinylidene fluoride (PVDF) membrane and probed with anti-His antibody (His-probe H-15, Santa Cruz Biotechnology Inc., 1:1000) for expression experiments or phospho-ERK 1/2 antibody (Cell Signaling Technology Inc., 1:1000 dilution) for MAPK studies. The phospho-ERK 1/2 membranes were stripped at 45 °C for 15 min in 62.5 mM Tris–HCl (pH 6.8) containing 1% SDS and 100 mM β-mercaptoethanol and washed extensively in TBST buffer before being reprobed with the anti-ERK 1/2 antibody (1:2000 dilution; Cell Signalling Technology). Blots were visualized by chemiluminescent substrate (LumiGLO Reserve; Kirkegaard & Perry Laboratories, Inc.) using a digital camera-based imaging system (Fluorchem 8000; Alpha Innotech Corporation).

2.10. Intracellular cAMP determination

Following infection for 48 h, cells were incubated with the phosphodiesterase inhibitor IBMX (0.5 mM) and then treated with varying concentrations of isoproterenol for 90 s before being lysed. Lysates were frozen at −80 °C and cAMP levels were determined in thawed cell lysates using the cAMP Biotrak Enzymeimmunoassay (EIA) system (GE healthcare, Baie d'Urfé, Québec, Canada) according to the manufacturer's instructions.

2.11. Phospholipase Cβ activity

Rat neonatal ventricular myocytes plated in 24-well dishes were incubated overnight with 37000 Bq ml^{-1} *myo*-[2-^{3}H]inositol (PerkinElmer Life Sciences) in serum-free DMEM (Invitrogen) [15]. The following day, unincorporated radioactivity was removed by washing the cells twice with Hanks' balanced salt solution (HBSS) (116 mM NaCl, 20 mM Hepes, 11 mM glucose, 5 mM $NaHCO_3$, 4.7 mM KCl, 2.5 mM $CaCl_2$, 1.3 mM $MgSO_4$, 1.2 mM KH_2PO_4, pH 7.4) containing 10 mM LiCl. Cells were then incubated for 15 min in HBSS containing 10 mM LiCl to inhibit inositol monophosphatase before treatment with increasing concentrations of agonist for 15 min at 37 °C. The reaction was stopped by lysing cells on ice with 0.8 M perchloric acid for 30 min, followed by neutralization of the lysates with 0.72 M KOH/0.6 M $KHCO_3$ solution. For each sample, total *myo*-[2-^{3}H]inositol incorporated into the cells was determined by counting the radioactivity present in 50 μl of the cell lysate. Inositol phosphates were recovered from the cell extracts by anion exchange chromatography using Dowex AG1-X8 (formate form), 200–400 dry mesh anion exchange resin (BioRad). The columns were loaded with 900 μl of the cell extract before successive washing with distilled water and 60 mM ammonium formate. Bound inositol phosphates were eluted with 1 M ammonium formate/0.1 M formic acid solution, and radioactivity was determined using a liquid scintillation counter. For each sample, the percent conversion of total *myo*-[2-^{3}H]inositol to [^{3}H]inositol phosphates was calculated. Cell density was monitored for each condition.

2.12. Cardiomyocyte siRNA transfection

Neonatal ventricular myocytes were transfected with siRNA 24 h after isolation using Lipofectamine 2000 reagent following the manufacturer's instructions (Invitrogen). Lipofectamine 2000 and siRNA were first separately diluted in OPTIMEM I (Invitrogen) and then mixed together at a v/v ratio of 4:1, Lipofectamine 2000 to siRNA. The cell culture medium was replaced with antibiotic-free transfection medium (DMEM/F12 and 2% fetal bovine serum) and following a 20 minute incubation at room temperature, the RNA-Lipofectamine 2000 mixture was added to the wells (150 pmol/well of a 6-well plate). Cells were maintained under normal conditions until analysis and the transfection medium was replaced with serum-free DMEM/F12 containing 1× ITS Liquid Media Supplement (Sigma-Aldrich®) 24 h after transfection.

2.13. Statistics

Group data are presented as mean ± S.E.M. for (n) determinations as indicated. Statistical significance was determined using one-way repeated measures ANOVA (GraphPad Prism 4) with Tukey's post-test. Normalized data were analyzed using column statistics followed by one-sample t test to determine if column means are significantly different than the hypothetical value of 100. Concentration-dependence data of cAMP accumulation was analyzed by nonlinear regression using a sigmoidal curve fit with a variable slope (GraphPad Prism 4). A p value <0.05 was considered statistically significant throughout.

3. Results

3.1. RGS2^{eb} expression attenuates the development of cardiomyocyte hypertrophy in response to phenylephrine and isoproterenol

Our previous work showed that full length RGS2 as well as the 37 amino acid residue eIF2B-interacting domain (RGS2^{eb}) can inhibit *de novo* protein synthesis *in vitro* as well as in multiple cell types. The ability of RGS2^{eb} to impede protein synthesis is sequence specific, as a control scrambled 37-mer peptide (same residues as RGS2^{eb} but in randomized order) did not exhibit any inhibitory effects on *in vitro* translation (data not shown). These results likely reflect the sequence and structural homology between RGS2^{eb} and the established eIF2B-binding region of aIF2β (bacterial homolog of eIF2β). Thus, we went on to examine whether RGS2 and RGS2^{eb} could also inhibit GPCR-stimulated protein synthesis and other indices of hypertrophy in isolated cardiomyocytes. Three major endpoints of hypertrophy were assessed: total cell surface area, rate of protein synthesis, and expression levels of genetic markers upregulated in the hypertrophic state. Adenoviral constructs [18] at an MOI of 10 achieved exogenous gene delivery to ≥95% of neonatal ventricular cells, with similar nuclear/cytosolic intracellular RGS2 and RGS2^{eb} distribution patterns and no apparent changes in cell morphology or viability (Fig. 1). Thus, all subsequent experiments involving viral-mediated gene delivery were performed at an MOI of 10. Following a 24 hour exposure, phenylephrine and isoproterenol both caused increases in cardiomyocyte cell size (Fig. 2A) and levels of protein synthesis (Fig. 2B), which is consistent with our previous studies [20,22]. These agonist-induced increases were almost completely blocked in cardiomyocytes overexpressing either RGS2 or RGS2^{eb}. Similarly, we tested whether RGS2^{eb} expression could also attenuate increases in the "fetal gene program", a group of key molecular markers associated with the hypertrophic phenotype including atrial natriuretic peptide (ANP), α-skeletal actin and β-myosin heavy chain (β-MHC). Both phenylephrine and isoproterenol were able to induce an increase in the level of α-skeletal actin, and phenylephrine treatment additionally resulted in increases in ANP and β-MHC, as measured by quantitative real-time PCR (Fig. 3). These increases were completely abrogated in cells infected with either RGS2 or RGS2^{eb} adenovirus.

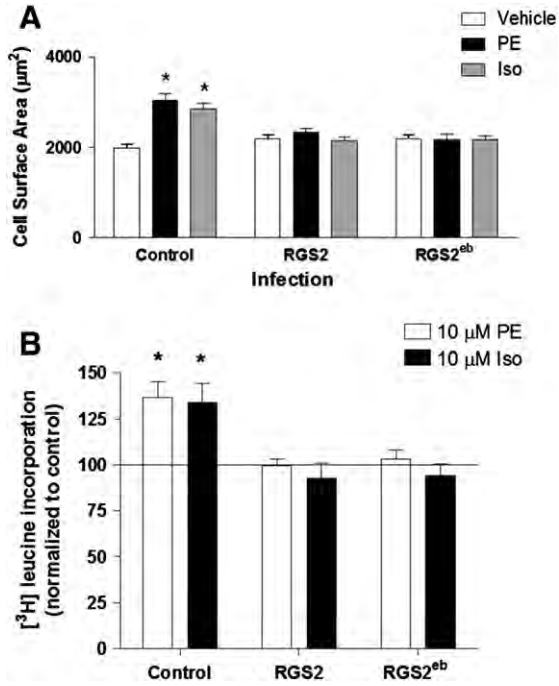

Fig. 2. The RGS2 eIF2B-binding domain blocks cardiomyocyte hypertrophy. NVM infected with either empty adenovirus (Control) or adenovirus encoding full-length RGS2 (RGS2) or the RGS2 eIF2B-binding domain (RGS2^{eb}) were treated with vehicle, phenylephrine (10 μM), or isoproterenol (10 μM) for 24 h. (A) Cells were then fixed and visualized, and cell surface area was assessed for 50 or more cells per condition. $n = 3$, error bars represent mean ± S.E.M., and $^*p < 0.05$ *versus* vehicle-treated, control infection. (B) NVM were incubated with [^{3}H]-leucine along with the indicated drugs for 24 h. Total protein was precipitated using 5% TCA and radiolabeled protein content was determined by scintillation counting. $n = 4$–6, done in quadruplicate. Error bars represent mean ±S.E.M. and $^*p < 0.05$ *versus* vehicle-treated, control infection.

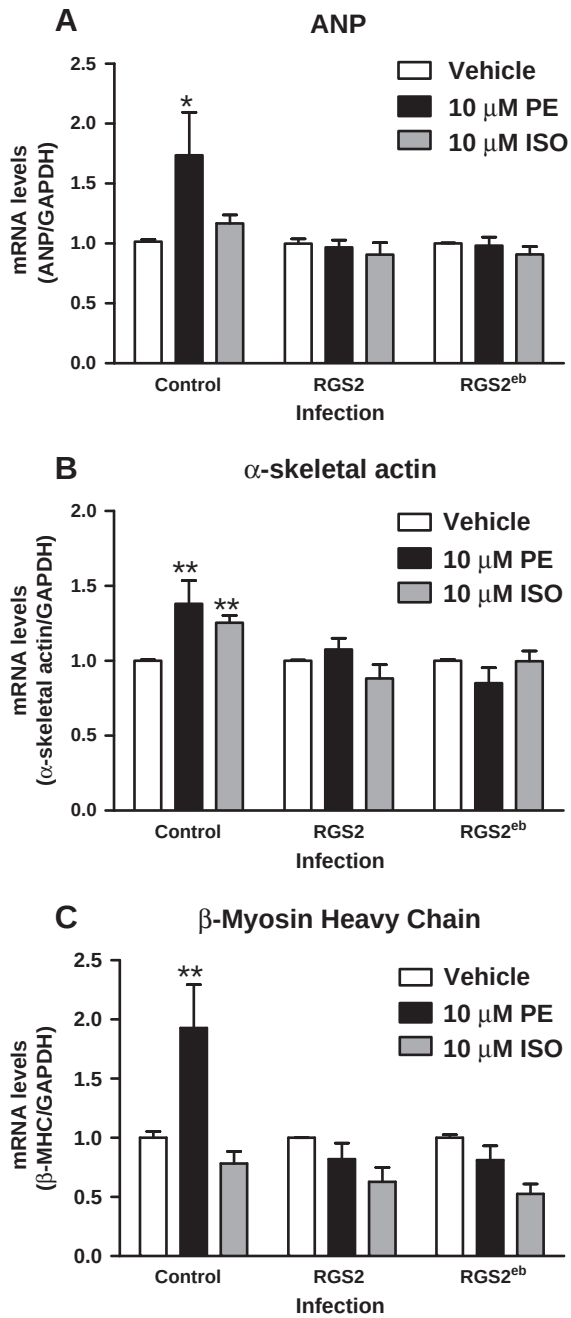

Fig. 3. The RGS2 eIF2B-binding domain blocks agonist-induced increases in genetic markers of hypertrophy. NVM infected with either empty adenovirus (Control) or adenovirus encoding full-length RGS2 (RGS2) or RGS2 eIF2B-binding domain (RGS2^{eb}) were treated with vehicle, phenylephrine (10 μM), or isoproterenol (10 μM) for 24 h. Expression levels of (A) ANP, (B) α-skeletal actin, and (C) β-MHC were determined using real-time PCR. mRNA levels were normalized to GAPDH mRNA and compared to vehicle treated values. $n = 3$–4, done in duplicate. Error bars represent mean ± S.E.M., $^{*}p < 0.05$, and $^{**}p < 0.01$ *versus* vehicle treated, Ad-Ctr.

3.2. RGS2^{eb} does not impair G protein-mediated signal transduction

Based on its structure, the eIF2B-binding domain of RGS2 would not be expected to enhance G protein GTP hydrolysis, and indeed, we failed to detect any effect of this domain on the GTPase activity of an M1 muscarinic receptor-Gα11 fusion protein in Sf9 cell membranes *in vitro*, whereas full length RGS2 and other B/R4 subfamily RGS proteins produced clear stimulatory effects [18]. However, RGS2 also can inhibit Gq-mediated phospholipase Cβ activity *via* GTPase-independent "effector antagonism" [28–30]; additionally it can inhibit Gs-stimulated adenylyl cyclase activity [15,22], although it does not alter Gs GTPase activity [11,14]. Therefore we examined the possible effects of RGS2^{eb} on GPCR-stimulated second messenger production in neonatal rat cardiomyocytes, as such effects could potentially contribute to its antihypertrophic function. Total inositol phosphate formation was measured as an indicator of PLCβ activity. RGS2 and RGS2^{eb} expression did not alter basal PLCβ activity as compared to control infected cells; however, upon receptor stimulation using phenylephrine, angiotensin II, or endothelin-1, inositol phosphate formation was significantly attenuated in cardiomyocytes expressing full-length RGS2 (Fig. 4A). This attenuation of PLCβ activity was absent from cells expressing RGS2^{eb} indicating that the eIF2Bε-binding region of RGS2 has no measurable effect on Gq/11-mediated signaling.

To determine whether the eIF2B-interacting domain of RGS2 might be capable of producing effects on Gs-mediated signal transduction, we measured isoproterenol-stimulated intracellular cAMP accumulation following infection with control, full-length RGS2, or RGS2^{eb} adenovirus. RGS2 overexpression was able to reduce the isoproterenol-induced, concentration-dependent increase in cAMP accumulation, producing a roughly four-fold increase in EC_{50}, whereas RGS2^{eb} expression had little or no effect (Fig. 4B). This result implies that the eIF2B-interacting domain of RGS2 does not inhibit isoproterenol-induced

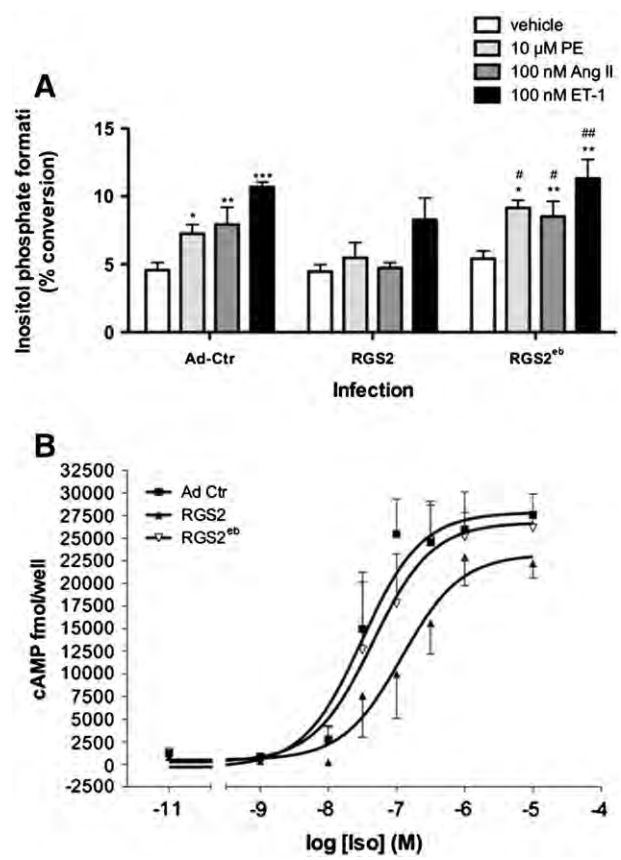

Fig. 4. The RGS2 eIF2B-binding domain does not affect Gs or Gq/11 signaling. (A) After infection with either Control, RGS2 or RGS2^{eb} adenovirus for 24 h, NVM were incubated with *myo*-[^{3}H]-inositol medium overnight, then stimulated with either vehicle, 10 μM phenylephrine, 100 nM angiotensin-II, or 100 nM endothelin-1 for 15 min. $n = 3$–4, performed in triplicate. Error bars represent mean ± S.E.M., $^{*}p < 0.05$ and $^{**}p < 0.01$ *versus* vehicle treated, Ad-Ctr; $^{\#}p < 0.05$ and $^{\#\#}p < 0.01$ *versus* RGS2^{eb} vehicle group. (B) NVM were infected with control (solid squares), RGS2 (upright triangles) or RGS2^{eb} (downward white triangles) adenovirus for 24 h, followed by treatment with isoproterenol at the indicated concentrations for 90 s. cAMP accumulation was assessed using a commercially available kit according to the manufacturer's instructions. $n = 3$, error bars represent mean ± S.E.M. Potency (pEC50) was significantly lower in RGS2-infected cells (7.502 ± 0.04, 6.848 ± 0.09, 7.348 ± 0.11 in Ad-Ctr, RGS2 and RGS2^{eb} respectively, $p = 0.05$).

cardiomyocyte hypertrophy *via* an inhibitory effect on adenylyl cyclase activity.

Mitogen-activated protein kinase signaling is thought to play a complex role in cardiac hypertrophy [31], and RGS2 has been shown to govern the effect of GPCRs and G proteins on MAP kinases including ERK 1/2, JNK and p38 [19,20,25]. Therefore, we examined the effects of RGS2 and its eIF2B-interacting domain on ERK 1/2 phosphorylation. As shown in Fig. 5, 10 min of stimulation with either phenylephrine or isoproterenol resulted in increased phosphorylation of ERK 1/2 in Ad-Ctr as well as in RGS2^{eb}-infected cells, whereas WT RGS2 overexpression clearly blunted ERK 1/2 activation. It thus appears that the protective effect of the RGS2 eIF2B-interacting domain does not involve the ERK 1/2 signaling pathway. Taken together, the results of Figs. 4 and 5 imply that the antihypertrophic effects of RGS2^{eb} do not involve any inhibitory effects on either G protein-dependent second messenger production or ERK 1/2 activation.

3.3. RGS2 knockdown augments agonist-stimulated protein synthesis in neonatal ventricular cardiomyocytes

In addition to examining overexpression of full length RGS2 on levels of protein synthesis in cultured neonatal ventricular myocytes, we also investigated whether cellular knockdown of RGS2 would produce the opposite effects, *i.e.* increasing rates of protein synthesis in these cells. Our initial work screened three commercially available RGS2 siRNA duplexes (Sigma-Aldrich) for their abilities to decrease RGS2 expression. After optimization of cell density/siRNA concentration/lipid carrier ratios, RGS2 knockdown of roughly 75% was achieved in cardiomyocytes using Lipofectamine-mediated transfection with one of the siRNA sequences (siRNA#3), as measured by qPCR (Fig. 6A). One other sequence (siRNA#1) produced no discernible change in RGS2 expression levels while an additional one (siRNA#2) produced an intermediate effect (data not shown), and these were not used in subsequent experiments. RGS2 siRNA#3, the most efficacious sequence, was tested for a functional effect on protein synthesis rates

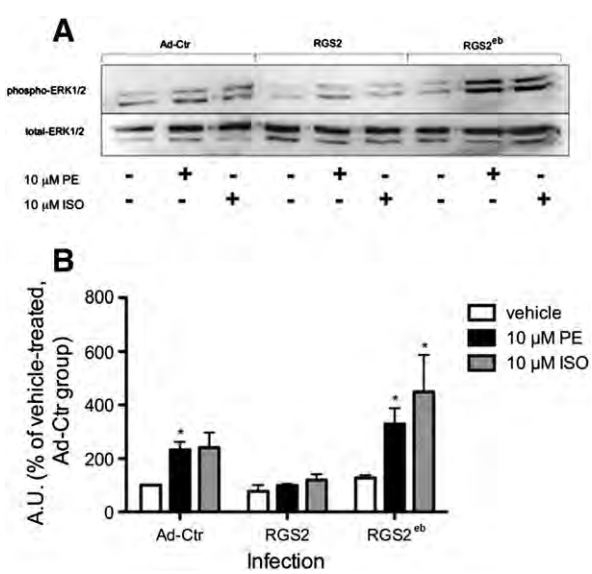

Fig. 5. The RGS2 eIF2B-binding domain does not interfere with ERK 1/2 phosphorylation. NVM were infected with Ad-Ctr, RGS2, or RGS2^{eb} adenovirus for 24 h, followed by treatment with vehicle, 10 μM phenylephrine, or 10 μM isoproterenol. Proteins in cell lysates were separated by SDS-PAGE and transferred to PVDF membrane, and the phosphorylation of ERK 1/2 was determined by Western blotting. The membranes were stripped and reprobed with anti-ERK 1/2 antibody. Shown is a representative of 4 independent experiments, the densitometric data of which are summarized in the bar graph in (B). Data are normalized to vehicle-treated, Ad-Ctr group and expressed as fold increase over control. $^{*}p < 0.05$ (matched-controls *vs.* treated group).

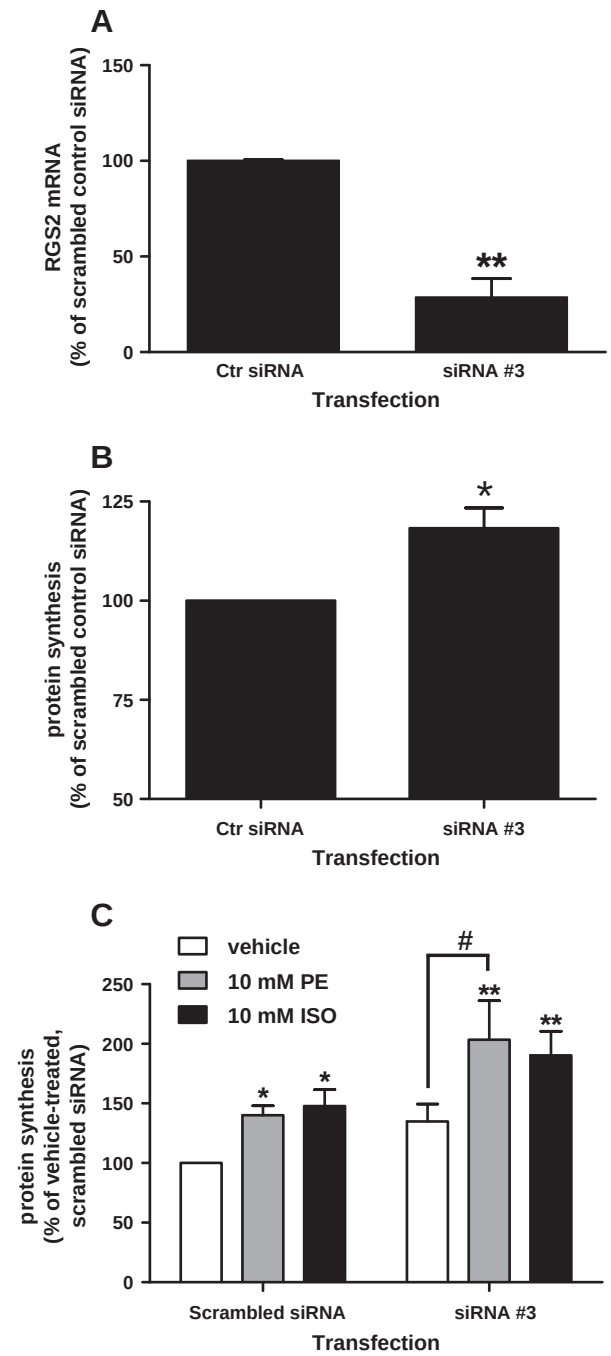

Fig. 6. Effect of siRNA-mediated RGS2 knockdown on protein synthesis in neonatal ventricular cardiomyocytes. (A) Scrambled control siRNA and an RGS2 siRNA sequence were transfected into NVM using Lipofectamine 2000 reagent for 24 h. RGS2 expression was then assessed by quantitative real time PCR. ($n = 4$, done in duplicate). (B) Following 24 hour transfection, NVM were incubated with 1 μCi/ml [^{3}H]-leucine for an additional 24 h to assess levels of protein synthesis ($n = 4$, done in quadruplicate). (C) Similarly, NVM were incubated with 1 μCi/ml [^{3}H]-leucine for an additional 24 h with either vehicle, 10 μM phenylephrine or 10 μM isoproterenol to assess levels of protein synthesis following hypertrophic stimulation ($n = 3$, done in sextuplicate). Error bars represent mean ±S.E.M., $^{*}p < 0.05$, and $^{**}p < 0.01$ *versus* scrambled or vehicle-treated, scrambled Ctr as indicated. $^{\#}p < 0.05$ *versus* RGS2 siRNA#3, vehicle-treated group.

in NVM by [^{3}H]-leucine incorporation and cells transfected with this showed a 20% increase in protein synthesis levels (Fig. 6B).

Lastly, we investigated whether stimulation with adrenergic agonists would further increase the hypertrophic response in cells with decreased RGS2. As expected, stimulation with phenylephrine and isoproterenol caused increased [^{3}H]-leucine incorporation, and

indeed, this was further increased in cardiomyocytes with reduced RGS2 (Fig. 6C). Taken together, these results suggest that a decrease in RGS2 is detrimental during a hypertrophic state, and are consistent with the interpretation that the ability of RGS2 to inhibit protein synthesis in neonatal ventricular myocytes is an important component of its antihypertrophic effect.

4. Discussion

The key finding of the present study is that cellular expression of the eIF2B-interacting domain of RGS2 is sufficient to impede the development of hypertrophy triggered by α1- and β-adrenergic agonists in neonatal cardiomyocytes, notwithstanding its lack of any measureable effect on second messenger production or ERK activation. Overexpression of full length RGS2, in contrast, inhibited both Gq- and Gs-mediated receptor signals as well as agonist-induced cardiomyocyte hypertrophy, while RGS2 knockdown resulted in increased *de novo* protein synthesis both in unstimulated cells and in those treated with the α1-adrenergic agonist phenylephrine.

RGS2 affects multiple signaling processes in cells of the heart [19,20,22,24,32–35], as well as other endpoints relevant to cardiovascular function including blood pressure [36], vascular tone [36], endothelial function [37], circulating catecholamine levels [38], and electrolyte/fluid excretion [21,39]. Although hearts from mice lacking RGS2 show no overt defects [40,41], such animals are highly sensitive to pressure-induced hypertrophy and heart failure [25] and several previous studies have shown RGS2 to impede cardiomyocyte hypertrophy induced by GPCR agonists [19,20,22,24]. The physiological and pathophysiological effects of RSG2 are generally attributed to its interactions with heterotrimeric G proteins and their associated signaling partners; however, the present results suggest that its interactions with eIF2Bε [18] are also important.

4.1. Antihypertrophic effects of RGS2 in cell-based assays

Cardiac hypertrophy is characterized principally by an increase in cardiomyocyte size, which necessarily reflects increased protein synthesis [6]. RGS2 has been shown to reduce protein synthesis in multiple cell types [18,23], and its ability to block agonist-induced increases in the incorporation of radiolabeled amino acids into neonatal rat cardiomyocytes tracks with its ability to inhibit GPCR agonist-induced increases in cell size [19,20,22,24,25].

Since RGS2 can inhibit both G protein-mediated signals as well as eIF2B activity, its ability to attenuate hypertrophy could result from either or both of these inhibitory effects, as illustrated in Fig. 7. The goal of the present study was to establish whether or not the ability of RGS2 to inhibit global protein synthesis might contribute to its observed ability to block GPCR agonist-induced cardiomyocyte growth. Biochemical cascades that promote hypertrophy in cardiomyocytes are triggered by Gq-coupled α1-adrenergic, angiotensin II, V1 vasopressin and endothelin-1 receptors and also β-adrenergic receptors, which couple mainly to Gs [5,6,42]. Multiple downstream kinases activated by these receptors converge on a conserved serine residue in GSK3β, the phosphorylation of which decreases the ability of this constitutively active kinase to act on multiple substrates including the ε-subunit of the initiation factor eIF2B. The phosphorylation of eIF2B limits its ability to activate eIF2, a rate-limiting step in mRNA translation [43]. Thus GPCR activation increases cell size by derepressing protein synthesis. Although G protein signaling also promotes other changes that increase the efficiency and capacity of mRNA translation (such as ribosome biogenesis) [3], the receptor-dependent decrease in eIF2B phosphorylation by GSK3β appears to be an essential step in isoproterenol-induced cardiomyocyte hypertrophy [27] and may be for other hypertrophic GPCR signals as well.

The present results show that eliminating the ability of RGS2 to block the activation of G protein effectors does not prevent it from

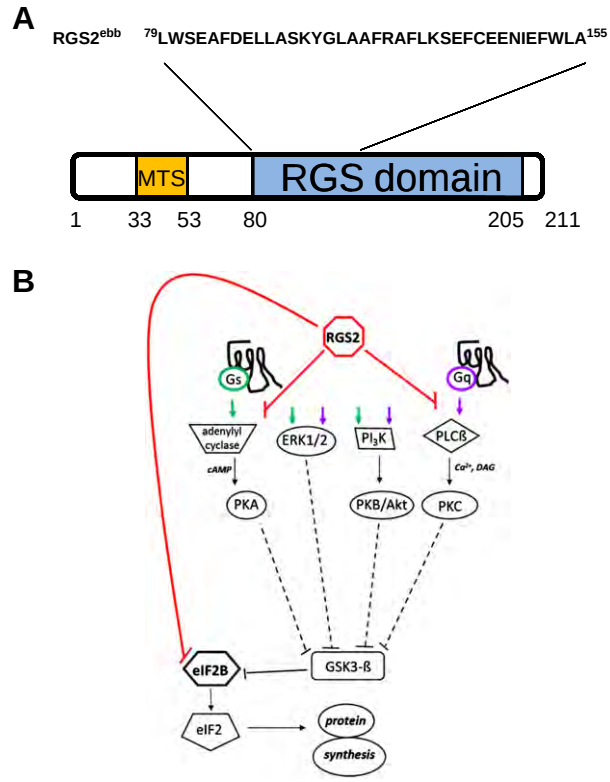

Fig. 7. RGS2 effects on GPCR-induced cardiomyocyte growth. (A) Domain structure of RGS2 and the sequence of the RGS2 eIF2Bε-binding domain. (B) The stimulation of GPCRs coupled to Gq or Gs activates multiple overlapping kinase cascades that target the constitutively active enzyme GSK3β, thereby decreasing its activity. This in turn leads to an increase in the ability of eIF2B to activate its binding partner eIF2 and promote protein synthesis and cell growth. RGS2 is able to inhibit GPCR-induced effector activation as well as eIF2B activity, and the present results show that the latter inhibitory effect is sufficient to impede GPCR-stimulated hypertrophy. MTS, membrane targeting sequence.

attenuating GPCR-induced cardiomyocyte hypertrophy. RGS2 can, as noted, target multiple points within the biochemical cascade that leads from GPCR activation to eIF2 activation, and disabling one of these interactions may potentially increase the utilization of the other. Thus, conversely it would be interesting to also determine whether selectively blocking the ability of RGS2 to inhibit mRNA translation had any impact on its ability to inhibit either Gq- or Gs-mediated hypertrophic effects. We were not able to identify any RGS2-based constructs lacking the ability to inhibit translation while retaining the ability to inhibit G protein-mediated signaling [18]; however, comparison with other R4/B subfamily RGS proteins suggests that the ability of RGS2 to inhibit Gq signaling likely contributes to its ability to impede the development of hypertrophy. The related proteins RGS4 and RGS5 can inhibit phenylephrine-stimulated protein synthesis in neonatal rat ventricular myocytes [19] even though they do not appear to directly inhibit protein synthesis ([18], Hong Ming and Peter Chidiac, unpublished observations). In the case of isoproterenol-induced cardiomyocyte hypertrophy, it is less clear whether the ability of RGS2 to inhibit Gs-stimulated adenylyl cyclase activity is important. In this and other studies RGS2 appeared to reduce agonist potency [22] but had little or no effect on maximal receptor-stimulated cAMP levels [19,22], and it follows that the inhibition of protein synthesis by RGS2 may play a more predominant role in this situation.

4.2. Effects on expression of hypertrophy-associated genes

The development of pathological cardiac hypertrophy is accompanied by the renewed expression of characteristic fetal genes, and similar transcriptional changes also occur in GPCR agonist-treated

cardiomyocytes [4]. We found that both RGS2 and RGS2^{eb} could block the agonist-induced upregulation of ANP, α-skeletal actin and β-MHC (Fig. 3), but the underlying mechanisms are uncertain.

GPCR-promoted expression of hypertrophy-associated genes is generally thought to result from the activation of calcineurin-dependent NFAT activation, triggered by Gq- or Gs-induced increases in cellular calcium [4]; RGS2^{eb} however did not block G protein-mediated signals in cardiomyocytes (Figs. 4 and 5) yet it still prevented markers of hypertrophy from increasing in response to G protein activation, suggesting that additional or alternative mechanisms of gene induction may be important. It has been proposed that reversion to the "fetal gene program" is a general response of the heart to stress [44], and in particular ER stress is characteristic of hypertrophic and failing hearts [5,45]. Hypertrophy-associated genes are upregulated in cardiomyocytes undergoing ER stress *via* calcineurin [46] and also *via* the transcription factor UPR-1, which is activated in response to the accumulation of misfolded proteins in the ER [47].

Treatment of isolated cardiomyocytes with angiotensin II [48], arginine vasopressin [49], or isoproterenol [50] leads to ER stress, while β-adrenergic receptor blocking drugs alleviate ER stress in animal models of heart failure [51]. Since ER stress can be relieved by reducing global protein synthesis [43], the present observations would appear to be consistent with a mechanism wherein inhibition of agonist-induced increases in gene expression by RGS2^{eb} reflects its ability to inhibit mRNA translation. It is well established that RGS2 is upregulated by various stimuli that promote ER stress, and thus its ability to reduce global protein synthesis may contribute to cell recovery [18,23]. It follows that the ability of RGS2^{eb}, as well as RGS2, RGS4 and RGS5 to impede agonist-promoted protein synthesis may be a key factor in reducing or preventing the genetic changes that accompany hypertrophy.

4.3. Antihypertrophic effects of RGS proteins in vivo

The enhanced degree of hypertrophy and increased incidence of heart failure that develop in RGS2 knockout animals that have undergone transverse aortic constriction [25] clearly point to a protective function of RGS2 *in vivo*; however many of the details of this beneficial effect remain to be elucidated. Although RGS2 is acutely and selectively upregulated in cardiomyocytes in response to Gq and Gs signaling [19,20,22], in the long-term RGS2 is downregulated *in vivo* in experimental hypertrophy and heart failure [24] but nonetheless a protective effect of RGS2 is still implied by comparison to animals completely lacking the protein [25].

The dwindling level of RGS2 in experimental hypertrophy suggests that optimal levels under pathological conditions may be lower than those under normal physiological conditions. Consistent with this idea, the targeted overexpression of RGS2 to the myocardium in transgenic mice did not provide any additional protection against hypertrophy [52]. In contrast, the targeted overexpression of either RGS4 [53] or RGS5 [54] to the myocardium has been shown to reduce cardiac hypertrophy. It may be noted that RGS2 is normally expressed at much higher levels than either RGS4 [55,56] or RGS5 [36,57] in the myocardium, and that RGS4 tends to be upregulated in heart failure [55,58]. Still, it is not clear why the targeted overexpression of RGS4 and RGS5 produced beneficial effects while RGS2 did not, as all three proteins appear to have the capability to inhibit G protein-mediated signals that promote hypertrophy. These three RGS proteins are not identical, however, and there may be varying selectivity among them for different pathogenic *versus* protective GPCR signaling pathways in cardiomyocytes. RGS2 also exhibits multiple properties not known to be shared by either RGS4 or RGS5 including nuclear localization [59], low affinity for Gαi/o [13], ability to inhibit Gs-stimulated adenylyl cyclase signaling [15], regulatory effects on several non-G protein targets [60], and the apparent ability to promote apoptosis [61]. The present results show that the eIF2B-interacting domain of RGS2 by itself can protect against hypertrophy at the cellular level, although further studies will be needed to determine whether such an effect might also contribute to the apparent ability of RGS2 to impede the progression of heart failure *in vivo*.

Conflict of interest

The authors declare no conflict of interest.

Acknowledgments

This work was supported by operating grants from the Canadian Institutes of Health Research and the Heart and Stroke Foundation of Ontario. PC was supported by a Career Investigator Award from the Heart and Stroke Foundation of Ontario. RG is supported by a New Investigator Award from the Heart and Stroke Foundation of Canada.

Appendix A. Supplementary data

Supplementary data to this article can be found online at http://dx.doi.org/10.1016/j.cellsig.2014.02.006.

References

[1] J.A. Hill, E.N. Olson, N. Engl. J. Med. 358 (2008) 1370.
[2] A. Diwan, G.W. Dorn II, Physiology (Bethesda) 22 (2007) 56.
[3] R.D. Hannan, A. Jenkins, A.K. Jenkins, Y. Brandenburger, Clin. Exp. Pharmacol. Physiol. 30 (2003) 517.
[4] N. Frey, E.N. Olson, Annu. Rev. Physiol. 65 (2003) 45.
[5] J.G. Dickhout, R.E. Carlisle, R.C. Austin, Circ. Res. 108 (2011) 629.
[6] G.W. Dorn II, T. Force, J. Clin. Invest. 115 (2005) 527.
[7] J. Heineke, J.D. Molkentin, Nat. Rev. Mol. Cell Biol. 7 (2006) 589.
[8] E.M. Ross, T.M. Wilkie, Annu. Rev. Biochem. 69 (2000) 795.
[9] M. Abramow-Newerly, A.A. Roy, C. Nunn, P. Chidiac, Cell. Signal. 18 (2006) 579.
[10] E.L. Riddle, R.A. Schwartzman, M. Bond, P.A. Insel, Circ. Res. 96 (2005) 401.
[11] T. Ingi, A.M. Krumins, P. Chidiac, G.M. Brothers, S. Chung, B.E. Snow, C.A. Barnes, A.A. Lanahan, D.P. Siderovski, E.M. Ross, A.G. Gilman, P.F. Worley, J. Neurosci. 18 (1998) 7178.
[12] W. Cladman, P. Chidiac, Mol. Pharmacol. 62 (2002) 654.
[13] S.P. Heximer, S.P. Srinivasa, L.S. Bernstein, J.L. Bernard, M.E. Linder, J.R. Hepler, K.J. Blumer, J. Biol. Chem. 274 (1999) 34253.
[14] A.A. Roy, K.E. Lemberg, P. Chidiac, Mol. Pharmacol. 64 (2003) 587.
[15] A.A. Roy, C. Nunn, H. Ming, M.-X. Zou, J. Penninger, L.A. Kirshenbaum, S.J. Dixon, P. Chidiac, J. Biol. Chem. 281 (2006) 32684.
[16] K. Heo, S.H. Ha, Y.C. Chae, S. Lee, Y.-S. Oh, Y.-H. Kim, S.-H. Kim, J.H. Kim, A. Mizoguchi, T.J. Itoh, H.M. Kwon, S.H. Ryu, P.-G. Suh, Cell. Signal. 18 (2006) 2182.
[17] J.P. Schoeber, C.N. Topala, X. Wang, R.J. Diepens, T.T. Lambers, J.G. Hoenderop, R.J. Bindels, J. Biol. Chem. 281 (2006) 29669.
[18] C.H. Nguyen, H. Ming, P. Zhao, L. Hugendubler, R. Gros, S.R. Kimball, P. Chidiac, J. Cell Biol. 186 (2009) 755.
[19] J. Hao, C. Michalek, W. Zhang, M. Zhu, X. Xu, U. Mende, J. Mol. Cell. Cardiol. 41 (2006) 51.
[20] M.-X. Zou, A.A. Roy, Q. Zhao, L.A. Kirshenbaum, M. Karmazyn, P. Chidiac, Cell. Signal. 18 (2006) 1655.
[21] A.M. Zuber, D. Singer, J.M. Penninger, B.C. Rossier, D. Firsov, J. Am. Soc. Nephrol. 18 (2007) 1672.
[22] C. Nunn, M.-X. Zou, A.J. Sobiesiak, A.A. Roy, L.A. Kirshenbaum, P. Chidiac, Cell. Signal. 22 (2010) 1231.
[23] C.H. Nguyen, P. Zhao, A.J. Sobiesiak, P. Chidiac, Biochem. Biophys. Res. Commun. 426 (1) (2012) 129–134.
[24] W. Zhang, T. Anger, J. Su, J. Hao, X. Xu, M. Zhu, A. Gach, L. Cui, R. Liao, U. Mende, J. Biol. Chem. 281 (2006) 5811.
[25] E. Takimoto, N. Koitabashi, S. Hsu, E.A. Ketner, M. Zhang, T. Nagayama, D. Bedja, K.L. Gabrielson, R. Blanton, D.P. Siderovski, M.E. Mendelsohn, D.A. Kass, J. Clin. Invest. 119 (2009) 408.
[26] P.H. Sugden, S.J. Fuller, S.C. Weiss, A. Clerk, Br. J. Pharmacol. 153 (Suppl. 1) (2008) S137.
[27] S.E. Hardt, H. Tomita, H.A. Katus, J. Sadoshima, Circ. Res. 94 (2004) 926.
[28] J.R. Hepler, D.M. Berman, A.G. Gilman, T. Kozasa, Proc. Natl. Acad. Sci. U. S. A. 94 (1997) 428.
[29] T. Anger, W. Zhang, U. Mende, J. Biol. Chem. 279 (2004) 3906.
[30] L.S. Bernstein, S. Ramineni, C. Hague, W. Cladman, P. Chidiac, A.I. Levey, J.R. Hepler, J. Biol. Chem. 279 (2004) 21248.
[31] I. Kehat, J.D. Molkentin, Circulation 122 (2010) 2727.
[32] A.K. Snabaitis, A. Muntendorf, T. Wieland, M. Avkiran, Cell. Signal. 17 (2005) 655.
[33] P. Zhang, J. Su, M.E. King, A.E. Maldonado, C. Park, U. Mende, Am. J. Physiol. Heart Circ. Physiol. 301 (2011) H147.
[34] J.M. Tuomi, P. Chidiac, D.L. Jones, Am. J. Physiol. Heart Circ. Physiol. 298 (2010) H554.
[35] K. Chakir, W. Zhu, S. Tsang, A.Y.-H. Woo, D. Yang, X. Wang, X. Zeng, M.-H. Rhee, U. Mende, N. Koitabashi, E. Takimoto, K.J. Blumer, E.G. Lakatta, D.A. Kass, R.-P. Xiao, J. Mol. Cell. Cardiol. 50 (2011) 1000.
[36] S. Gu, C. Cifelli, S. Wang, S.P. Heximer, Clin. Sci. 116 (2009) 391.

[37] P. Osei-Owusu, R. Sabharwal, K.M. Kaltenbronn, M.-H. Rhee, M.W. Chapleau, H.H. Dietrich, K.J. Blumer, J. Biol. Chem. 287 (2012) 12541.
[38] J. Tank, M. Obst, A. Diedrich, R.J. Brychta, K.J. Blumer, K. Heusser, J. Jordan, F.C. Luft, V. Gross, Auton. Neurosci. 136 (2007) 52.
[39] S.B. Gurley, R.C. Griffiths, M.E. Mendelsohn, R.H. Karas, T.M. Coffman, J. Am. Soc. Nephrol. 21 (2010) 1847.
[40] S.P. Heximer, R.H. Knutsen, X. Sun, K.M. Kaltenbronn, M.-H. Rhee, N. Peng, A. Oliveira-dos-Santos, J.M. Penninger, A.J. Muslin, T.H. Steinberg, J.M. Wyss, R.P. Mecham, K.J. Blumer, J. Clin. Invest. 111 (2003) 445.
[41] C. Nunn, P. Zhao, M.-X. Zou, K. Summers, C.G. Guglielmo, P. Chidiac, Cell. Signal. 23 (2011) 1375.
[42] S.E. Hardt, J. Sadoshima, Cardiovasc. Res. 63 (2004) 500.
[43] R.C. Wek, H.-Y. Jiang, T.G. Anthony, Biochem. Soc. Trans. 34 (2006) 7.
[44] M. Rajabi, C. Kassiotis, P. Razeghi, H. Taegtmeyer, Heart Fail. Rev. 12 (2007) 331.
[45] J. Groenendyk, P.K. Sreenivasaiah, D.H. Kim, L.B. Agellon, M. Michalak, Circ. Res. 107 (2010) 1185.
[46] Z.-Y. Zhang, X.-H. Liu, W.-C. Hu, F. Rong, X.-D. Wu, Am. J. Physiol. Heart Circ. Physiol. 298 (2010) H1499.
[47] T. Sawada, T. Minamino, H.Y. Fu, M. Asai, K. Okuda, T. Isomura, S. Yamazaki, Y. Asano, K. Okada, O. Tsukamoto, S. Sanada, H. Asanuma, M. Asakura, S. Takashima, M. Kitakaze, I. Komuro, J. Mol. Cell. Cardiol. 48 (2010) 1280.
[48] X.-J. Zou, L. Yang, S.-L. Yao, Exp. Biol. Med. (Maywood) 237 (2012) 1341.
[49] M.A. Brostrom, F. Mourad, C.O. Brostrom, J. Cell. Biochem. 83 (2001) 204.
[50] S. Dalal, C.R. Foster, B.C. Das, M. Singh, K. Singh, Mol. Cell. Biochem. 364 (2012) 59.
[51] L. Ni, C. Zhou, Q. Duan, J. Lv, X. Fu, Y. Xia, D.W. Wang, PLoS ONE 6 (2011) e27294.
[52] C. Park-Windhol, P. Zhang, M. Zhu, J. Su, L. Chaves Jr., A.E. Maldonado, M.E. King, L. Rickey, D. Cullen, U. Mende, PLoS ONE 7 (2012) e40048.
[53] J.H. Rogers, P. Tamirisa, A. Kovacs, C. Weinheimer, M. Courtois, K.J. Blumer, D.P. Kelly, A.J. Muslin, J. Clin. Invest. 104 (1999) 567.
[54] H. Li, C. He, J. Feng, Y. Zhang, Q. Tang, Z. Bian, X. Bai, H. Zhou, H. Jiang, S.P. Heximer, M. Qin, H. Huang, P.P. Liu, C. Huang, Proc. Natl. Acad. Sci. U. S. A. 107 (2010) 13818.
[55] C. Mittmann, C.H. Chung, G. Höppner, C. Michalek, M. Nose, C. Schüler, A. Schuh, T. Eschenhagen, J. Weil, B. Pieske, S. Hirt, T. Wieland, Cardiovasc. Res. 55 (2002) 778.
[56] C. Larminie, P. Murdock, J.-P. Walhin, M. Duckworth, K.J. Blumer, M.A. Scheideler, M. Garnier, Brain Res. Mol. Brain Res. 122 (2004) 24.
[57] C.A. Doupnik, T. Xu, J.M. Shinaman, Biochim. Biophys. Acta 1522 (2001) 97.
[58] V.J. Owen, P.B. Burton, A.J. Mullen, E.J. Birks, P. Barton, M.H. Yacoub, Eur. Heart J. 22 (2001) 1015.
[59] P. Chidiac, A.A. Roy, Recept. Channels 9 (2003) 135.
[60] N. Sethakorn, D.M. Yau, N.O. Dulin, Cell. Signal. 22 (2010) 1274.
[61] M. Endale, S.D. Kim, W.M. Lee, S. Kim, K. Suk, J.Y. Cho, H.J. Park, Y. Wagley, S. Kim, J.-W. Oh, M.H. Rhee, Am. J. Physiol. Cell Physiol. 298 (2010) C611.